Salicylaldehyde hydrazones: buttressing of outer sphere hydrogen bonding and copper extraction properties.

Tai Lin, Heiko Bauer, Ross S Forgan, Simon Parsons, David M Rogers, Benjamin D Roach, Fraser J White and PAT*

Abstract

Salicylaldehydes hydrazones are weaker copper extractants than their oxime derivatives which are used in hydrometallurgical processes to recover approximately 20% of the world's copper. Their strength, based on the extraction equilibrium constant K_e, can be increased by nearly three orders of magnitude by incorporating electron-withdrawing or hydrogen bond acceptor groups (X) *ortho* to the phenolic OH group of the salicylaldehyde unit. DFT calculations suggest that the effects of the 3-X substituents arise from a combination of their influence on the acidity of the phenol in the pH-dependent equilibrium:

$$Cu^{2+} + 2LH_{org} \rightleftharpoons [CuL_2]_{org} + 2H^+ \qquad \textbf{Equation 1}$$

and on their ability to "buttress" interligand hydrogen bonding by interacting with the hydrazone N-H donor group. X-ray crystal structure determination and computed structures indicated that in both the solid state and the gas phase, coordinated hydrazone groups are less planar than coordinated oximes and this has an adverse effect on intramolecular hydrogen bond formation to the neighbouring phenolate oxygen atoms.

Introduction

Approximately 20% of the world's copper is produced hydrometallurgically using phenolic oxime solvent extractants[1, 2] of the types[3, 4] shown in Figure 1. The acidity of the phenol allows metal uptake and release to be controlled by varying the pH of the aqueous phase (see Figure 1).

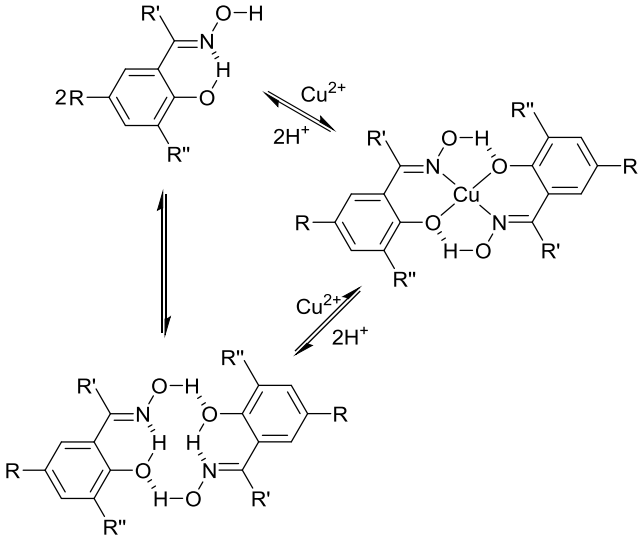

Figure 1 The pH-dependent complexation of copper(II) by phenolic oxime extractants

The high selectivity for Cu(II) over other 1st transition series metal cations has been

assumed to be due, at least in part, to the goodness-of-fit[5] for the cavity in these pseudomacrocyclic ligands. The head-to-tail hydrogen bonding in the complexes is also often found in the free ligands. [5]

In principle, variation of R, R' or R'' groups in the structure in Figure 1 can be used to tune the extractant strength, which is usually defined for these systems by the $pH_{0.5}$ values (the pH at which 50% of the theoretical loading is observed). Variation of the nature of an alkyl group *para* to the phenol (R in Figure 1) does not change $pH_{0.5}$ values greatly,[3, 6, 7] but more highly branched alkyl groups impart higher solubility in the hydrocarbon diluents used in industrial applications.

In general salicylaldoximes with R' = H are stronger extractants than ketoximes or benzophenone oximes where R' groups are alkyl or aromatic groups.[3] Groups present in the 3-position, *ortho*- to the phenolic oxygen atom (R'' in Figure 1), have very significant effects on extractant strength.[3,6-8] Electron-withdrawing substituents such as halide and nitro groups make the ligands more acidic, favouring the extraction equilibrium shown in Equation 3; while electron-donating substituents such as alkyl and methoxy groups have the opposite effect.[3, 8] Although ligands with higher phenol acidity form conjugate phenolate ions with lower basicity, which are poorer σ-donors[9] and will give a smaller overall formation constant β_2, the square dependence of K_e on K_a:,

$$K_e \rightleftharpoons \beta_2 K_a^2 \qquad \textbf{Equation 2}$$

where K_e is the equilibrium constant for the formation of the neutral complex in a single phase,

$$Cu^{2+} + 2LH \rightleftharpoons [CuL_2] + 2H^+ \qquad \textbf{Equation 3}$$

β_2 represents the overall formation constant for the 2:1 (ligand : Cu^{II}) complex,

$$Cu^{2+} + 2L^- \rightleftharpoons [CuL_2] \qquad \textbf{Equation 4}$$

and K_a represents the acid dissociation constant of the ligand LH,

$$LH \rightleftharpoons L^- + H^+ \qquad \textbf{Equation 4}$$

indicates that the phenol acidity has a greater effect on K_e than the phenolate basicity.

Substituents in the 3-position also influence the inter-ligand hydrogen-bonding shown in Figure 1. Bulky *t*-butyl groups disrupt this stabilising motif, whilst hydrogen bond acceptors such as halide, nitro and methoxy groups favour formation of bifurcated hydrogen bonds,[10] "*buttressing*" the stabilising motif,[6, 7] and thus increasing extractant strength.

The combination of electronic, steric and hydrogen-bond buttressing effects underpin the observed variation of by more than two orders of magnitudes of the distribution coefficients for copper in the series of 3-substituted 3-*tert*-butylsalicylaldoxime extractants: Br > NO_2 > Cl > OMe > Me ≥ H > ^{t}Bu.[6, 7]

Salicylaldehyde hydrazones (Figure 2) could also form N-H···O hydrogen bonds to

generate dimers with a $R_4^4(10)$ graph set descriptor[11] and thus yield pseudomacrocyclic complexes similar to those formed by the analogous oximes. In this paper we consider whether 3-substitution of the phenol ring or *N*-substitution of the hydrazone group can be used to tune extractant strength to meet the requirements of commercial operations. It has been reported that both the unsubstituted ligand with R = R' = X = H (Figure 2) and its *N*-phenyl analogue (R = X = H, R' = C_6H_5) form neutral complexes of the type [Cu(**L**-H)$_2$].[12-16]

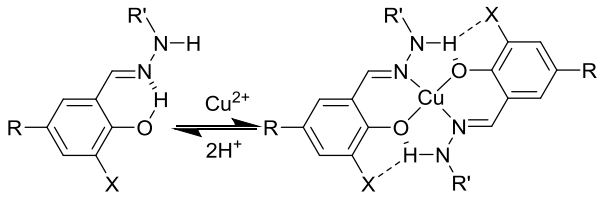

	L1	L2	L3	L4	L5	L6	L7	L8	L9	L10
X	H	Me	NO_2	Br	OMe	H	Me	NO_2	Br	OMe
R	Me	Me	Me	Me	Me	Ph	Ph	Ph	Ph	Ph
R'	^{t}Bu	^{t}Bu	^{t}Bu	^{t}Bu	^{t}Bu	^{t}Bu	^{t}Bu	^{t}Bu	^{t}Bu	^{t}Bu

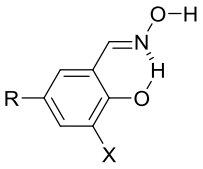

	O1	O2	O3	O4	O5
X	H	Me	NO_2	Br	OMe
R	^{t}Bu	^{t}Bu	^{t}Bu	^{t}Bu	^{t}Bu

Figure 2 The 3- and N-substituted salicylaldehyde hydrazones **L1**-**L10** and their pseudomacrocyclic copper complexes [Cu(**L**-H)$_2$], and related salicylaldoxime extractants **O1**-**O5** discussed in this paper.

No work has been reported on the use of salicylaldehyde hydrazones as copper extractants, but other types of hydrazones have been used as spectrophotometric and gravimetric reagents for the detection and analysis of transition metals, including copper, nickel and iron.[12, 13, 17] Some show unusual magnetic[18, 19] and electronic[20] properties, or are nonlinearly optically active[21-23] or fluorescent[24, 25] materials. They can also be used as optical chemosensors for analytical purposes.[26, 27] Salicylaldehyde benzoylhydrazone and analogous aroyl hydrazones have been studied as chelating agents to mobilize iron for iron-overload therapy,[28, 29] and their transition metal complexes possess antitumour properties.[30-33] Many hydrazones and their transition metal complexes are used as antibacterial, antiviral, antitubercular,[34] antimycobacterial[35] and antifungal agents,[36, 37] and in industry they are employed as plasticizers[38] and catalysts.[39-41]

N-acyl and *N*-aroyl hydrazones of salicylaldehyde[42-46] (Figure 3) can form 2:2 copper(II) complexes as tridentate ligands with the phenolate oxygen, azomethine nitrogen and enolimide oxygen atoms defining the binding site.[42-46] In the *N*-aroylhydrazones shown in Figure 3 it is understood[42-46] that the phenolate oxygen atoms act as the bridges between the two copper atoms and in some cases a solvent

molecule acts as a fifth ligand for each copper atom.

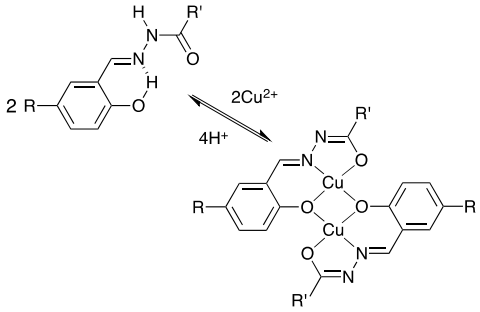

Figure 3 Dinuclear complexes formed by *N*-acyl or *N*-aroyl hydrazones of salicylaldehyde derivatives.[42-48]

The 2Cu:2L stoichiometry and 3Cu:2L stoichiometry of related systems has been exploited to enhance the mass transport efficiency of copper extraction over that associated with the 1Cu:2L system currently used (Figure 1) in commercial processes.[47, 48]

Results and Discussion

L1-**L10** were readily obtained in high yields (see ESI) by reaction of methyl or phenyl hydrazine with the substituted salicylaldehydes **1**-**5** which were prepared by formylation and 3-substitution of 4-*tert*-butylphenol (Scheme 1). A stock of 5-*tert*-butyl-2-hydroxybenzaldehyde (**1**) was synthesized by the Levin method,[49] and the nitro-substituted (**3**) and bromo-substituted (**4**) salicylaldehydes were produced by optimizing literature conditions for electrophilic substitution.[50] The methoxy-substituted salicylaldehyde (**5**) was prepared from its bromo analogue **4** by a modification of the literature method.[51] In the case of 3-methyl-salicylaldehyde (**2**), the synthesis exploited the modified Duff reaction[52] starting with 4-*tert*-butyl-2-methylphenol, since it was commercially available and it would be difficult to methylate **1** by Friedel-Crafts or related reactions.

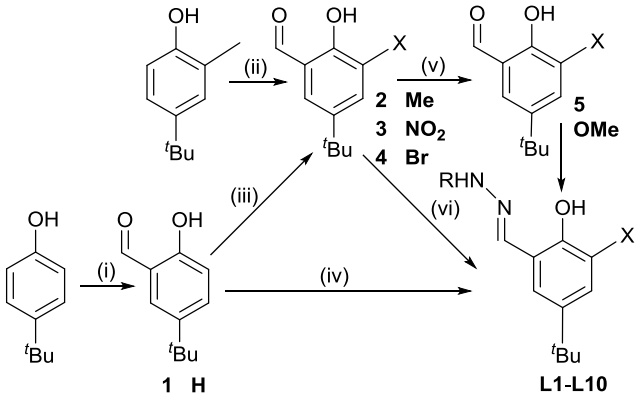

Scheme 1 Synthetic routes to salicylaldehyde hydrazones **L1**-**L10**.

X-ray structure determinations of **L6** and **L10** (Figure 4) reveal that, as expected, the phenolic group acts as an intramolecular bond donor, O-H···N, to the imine nitrogen atom and as an intermolecular hydrogen bond acceptor from a hydrazone NH group in a neighbouring molecule. In both structures the hydrogen bonding involving the NH groups leads to the formation of linear polymers rather than pseudomacrocyclic dimers

of the type commonly found[5] in the structures of phenolic oximes (see Figure 1) which are preorganised for metal binding. In the case of **L10** the formation of the linear polymer is clearly favoured by the hydrazone group being able to make an additional bonding contact with the 3-methoxy group.

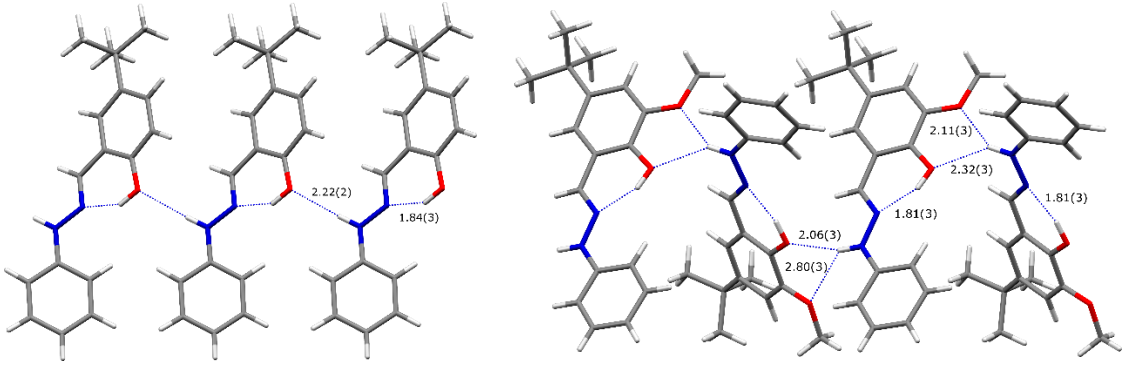

Figure 4. X-ray crystal structures of the free ligands **L6** and **L10** with hydrogen bond distances/Å.

NMR methods were used to probe how tautomerism, phenol acidity, hydrogen bonding and intermolecular association in solution (Figure 2) are affected by the substituents on the nitrogen atom or *ortho*- to the phenol (Y or X respectively in Figure 5) because these are likely to have a significant influence on strength as metal extractants. The ^{1}H NMR spectra confirm (see ESI) that the ligands exist in solution as the imino-enol tautomer (Figure 5) as expected from the substantial advantage of aromaticity.[53,54]

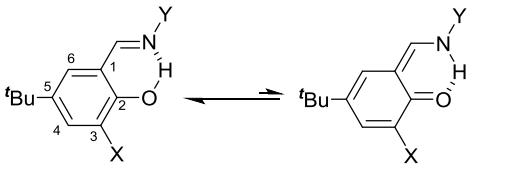

X = H, Me, NO_2, Br, OMe and Y = OH, NHMe, NHPh

Figure 5 Imino-enol and amino-keto tautomers of the structurally related salicylaldoximes (**O1**-**O5**), *N*-methylhydrazones (**L1**-**L5**) and *N*-phenylhydrazones (**L6**-**L10**).

All the resonances in the ^{1}H NMR spectra of the *N*-methylhydrazones **L1**-**L5**, and the *N*-phenylhydrazones **L6**-**L10**, can be unambiguously assigned. In the spectra of the *N*-methylhydrazones, the hydrazone proton is coupled with the NC*H*$_3$ protons and appears as a quartet at δ = 7-8 ppm (ESI). For the *N*-phenylhydrazones **L6**-**L10**, both the phenol and hydrazone protons appear as singlets at $\delta > 10$ ppm. These can be distinguished by examining the COSY spectra which indicate a weak coupling between the azomethine proton and one of the very low field protons (Figure S1) which was therefore assigned as the hydrazone.

For the oximes **O1**-**O5**, the COSY spectra did not show spin-spin coupling between the azomethine and oxime protons, which suggests that the oxime oxygen, in contrast with the methyl hydrazone NH group, is not much involved in the conjugation of the molecule. Heteronuclear Multiple Bond Connectivity (HMBC, also known as long-range ^{1}H-^{13}C COSY) experiments were carried out to distinguish the phenol and oxime

protons. The HMBC spectrum of the unsubstituted oxime **O1** in DMSO-d_6 (Figure S2) reveals correlation between the azomethine ^{13}C at 148.95 ppm and the proton at 11.25 ppm, which confirms the latter to be the oxime proton.

An order of electron-withdrawing effect, oxime > phenylhydrazone > methylhydrazone, is supported by the comparison of ^1H NMR spectra of the unsubstituted ligands **L1**, **L6** and **O1** with 4-*tert*-butylphenol, and those of the 3-methyl substituted ligands **L2**, **L7** and **O2** with 4-*tert*-butyl-2-methyl-phenol (see ESI). It has been shown[55, 56] that there is a linear correlation between the pK_a values of phenols in aqueous solution and the chemical shift of the phenolic protons at infinite dilution in DMSO. On this basis, the chemical shift data for **L1**-**L10** and **O1**-**O5** in DMSO-d_6 (Table 1) suggest that the acidity of the phenolic proton follows the electron-withdrawing properties of the imine component with oxime > phenylhydrazone > methylhydrazone. The effect of the 3-substituent effects on acidity: NO_2 > Br > Me > H > OMe also follows that expected from their electron-withdrawing properties.

3-Substituent	Methylhydrazones		Phenylhydrazones		Oximes	
H	**L1**	11.19	**L6**	10.40	**O1**	9.88
Me	**L2**	11.57	**L7**	11.09	**O2**	10.12
NO_2	**L3**	12.94	**L8**	11.76	**O3**	11.13
Br	**L4**	12.26	**L9**	11.64	**O4**	10.69
MeO	**L5**	11.08	**L10**	9.99	**O5**	9.48

Table 1 Chemical shifts of the phenolic hydrazone and oxime protons of **L1**-**L10** and **O1**-**O5** in DMSO-d_6

Hydrogen bonding between ligands in solution, to form cyclic dimers or linear oligomers, is of great relevance to ligand preassembly and strength as metal extractants. The temperature and concentration dependence of ^1H NMR experiments (ESI Figure S3) show that, in contrast to the CH protons, the shifts for the phenolic and oximic protons are markedly temperature dependent. As temperature is increased the larger shift of the hydrazone signal to high field compared to that of the phenol is consistent with the former forming inter- and the latter intra-molecular hydrogen bonds.[57-61] The preference for the phenolic proton to form an intramolecular hydrogen bond to the imino nitrogen accords with solid state structures (see Figure 4). An exception is the 3-nitrosubstituted ligands where the nitro-group competes effectively for the phenolic proton to give structures such as those shown in Figure 6 (see also computational results below).

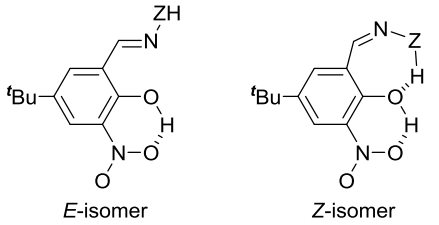

Figure 6 The *E* and *Z* isomers of the 3-nitrosubstituted ligands **L3**, **L8** and **O3** in which ZH = MeNH, PhNH and OH

The conformation and aggregation of the methylhydrazones **L1-L5** were investigated by Nuclear Overhauser Effect Spectroscopy (NOESY). The spectrum of **L2** in $CDCl_3$ (Figure 7) demonstrates that the azomethine proton is close to both the N-substituted methyl group and the benzene's 6 proton. This is consistent with the presence of a phenol OH to imino N intramolecular hydrogen bond in the *E* conformation (see Figure 8).

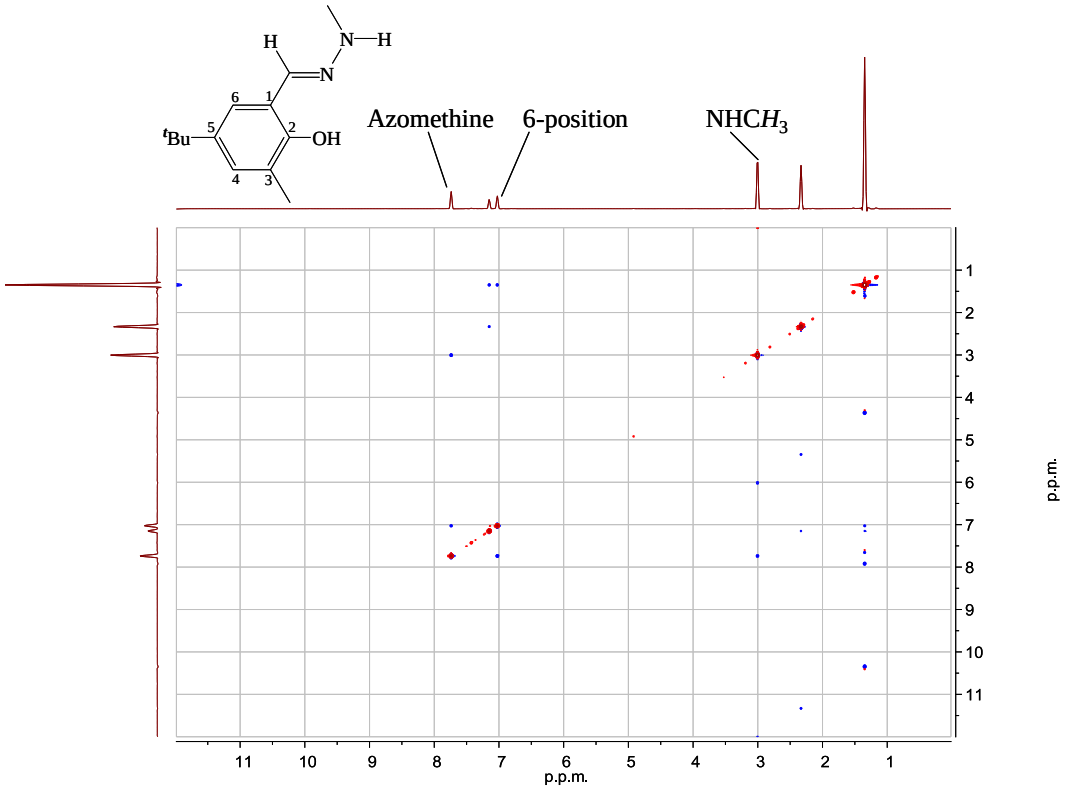

Figure 7 NOESY spectrum of **L2** in $CDCl_3$

The *E* conformation implied by the NOESY spectrum allows the pseudomacrocyclic dimer to be formed as shown in Figure 8.

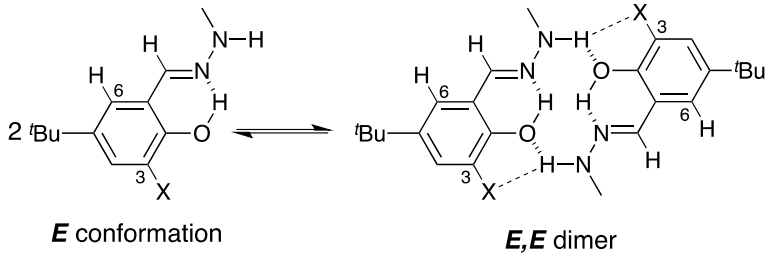

Figure 8 Formation of cyclic dimers from the *E* conformers of the salicylaldehyde methylhydrazones showing possible hydrogen bond buttressing by the 3-X groups.

The NMR results suggest that in solution the hydrazone proligands **L1-L10** show a similar facility for aggregation and preorganisation to their much more studied oxime analogues. Consequently their abilities to function as extractants for Cu^{II} are of interest.

All the hydrazone proligands were found to form 1:2 Cu:L complexes [Cu(**L**-H)$_2$] on reaction with copper(II) acetate in methanol. X-ray structure determinations of [Cu(**L1**-H)$_2$] and [Cu(**L5**-H)$_2$] confirm that the methylhydrazones yield planar Cu(II) complexes with pseudomacrocyclic structures similar to their oxime analogues (Figure 9). The intramolecular contacts between terminal hydrazone nitrogen atoms and the phenolate oxygen atoms, $Y^1\cdots O^2$ in the hydrazone complexes are slightly longer than those defining the intramolecular hydrogen bond in the oxime complex [Cu(**O1**-H)$_2$] (see Table 2).

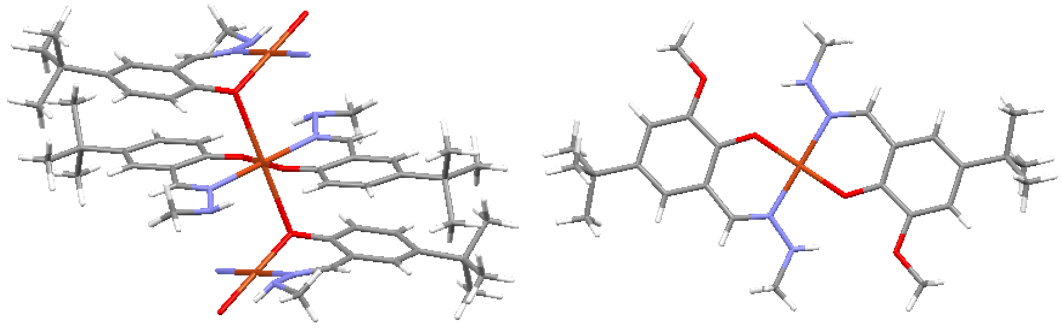

Figure 9 The solid state structures of [Cu(**L1**-H)$_2$] (left) and [Cu(**L5**-H)$_2$] (right).

The Cu-N and Cu-O bond lengths in the hydrazone complexes (Table 2) fall in a similar range to those found in the related oxime complexes.[5] As the structures all have the copper atom or a crystallographic inversion centre the *bonding cavity radius*[5] defined by the N_2O_2 set is the mean of the Cu-O and Cu-N lengths. The smaller value for the oxime complex [Cu(**O1**-H)$_2$] implies tighter binding than in the hydrazone complexes but caution needs to be exercised in using cavity radii determined from solid state structures to compare the equatorial planar fields defined by the N_2O_2 donor sets because axial contacts vary considerably between structures,[5] for example the phenolate oxygen atoms of an adjacent complex make close contacts in the structure of [Cu(**L1**-H)$_2$] (see Figure 9) but not in [Cu(**L5**-H)$_2$].

Compound	X	Y	R
[Cu(**L1**-H)$_2$]	H	N	Me
[Cu(**L5**-H)$_2$]	OMe	N	Me
[Cu(**O1**-H)$_2$]	H	O	-

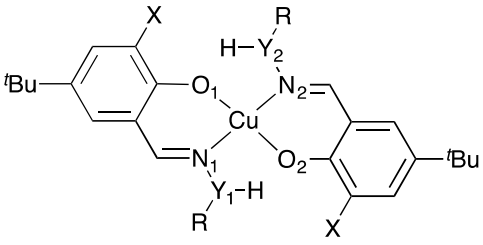

Bond lengths/Å and angles/°[a]	[Cu(**L1**-H)$_2$] PT0006	[Cu(**L5**-H)$_2$] PT0002	[Cu(**O1**-H)$_2$] PT0532		
Cu-O$_1$	1.9244(11)	1.8658(10)	1.905(2)	1.900(2)	1.907(2)
Cu-N$_1$	1.9986(13)	2.0020(13)	1.941(2)	1.945(2)	1.943(2)
O$_1$-Cu-O$_2$	180.0	180.0	180.0	180.0	180.0
N$_1$-Cu-N$_2$	180.0	180.0	180.0	180.0	180.0
O$_1$-Cu-N$_1$	91.03(5)	92.24(5)	92.26(8)	92.13(8)	91.76(8)
O$_2$-Cu-N$_1$	88.97(5)	87.76(5)	87.74(8)	87.87(8)	88.24(8)
Y$_1$···O$_2$	2.7005(18)	2.604(4) 2.614(4)	2.581(2)	2.583(5)	2.584(3)
Cavity radius[b]	1.962(2)	1.934(2)	1.923(3)	1.923(3)	1.925(3)
O$_1$-Cu-N$_1$-Y$_1$	160.55(10)	168.7(2) 162.8(2)	173.8(2)	177.9(2)	175.5(2)
O$_2$-Cu-N$_1$-Y$_1$	19.45(10)	11.3(2) 17.2(2)	6.20(16)	2.12(16)	4.54(16)
Distance of Y from CuN$_2$O$_2$ plane	0.418(1)	0.247(2) 0.380(4)	0.135(2)	0.046(2)	0.099(2)

Table 2 Bond lengths/Å and angles/° in the inner coordination spheres of the [Cu(**L1**-H)$_2$] and [Cu(**L5**-H)$_2$] compared with those in [Cu(**O1**-H)$_2$]. [a] In all complexes the Cu^{II} atom lies on an inversion centre. [b] The mean distance of the donor N and O atoms from their centroid.

An interesting feature of the structures of [Cu(**L1**-H)$_2$] and [Cu(**L5**-H)$_2$] is that the hydrazone N-N bonds bend away from the central CuN$_2$O$_2$ unit to a greater extent than the N-O bonds in the related oxime complexes. This is manifest (Table 2) by larger deviations of the terminal hydrazone nitrogen atoms from the least squares planes defined by copper atom and the donor set (CuN$_2$O$_2$) than the oximic oxygen atoms and by the related torsion angles. The implications of this are that *inter*-ligand hydrogen bonding is weaker in the hydrazones and will reduce complex stability and extractant strength. This and the effects on the hydrogen bonding by the 3-X substituents are considered further in DFT calculations (see below).

A preliminary investigation of the strength of the hydrazones as solvent extractants by studying the pH-dependence of the reaction,

$$CuSO_4 + 2L_{(CHCl_3)} \rightleftharpoons [Cu(L-H)_2]_{(CHCl_3)} + H_2SO_4 \qquad \textbf{Equation 5}$$

indicated that they are intrinsically weaker extractants than their oxime analogues. Two problems were encountered in obtaining solvent extraction data. For some of the weaker extractants loading only occurred at pH values at which precipitation of copper(II) hydroxide occurs and several of the ligands and their Cu(II) complexes were insufficiently soluble in chloroform to allow extraction experiment to be conducted. To circumvent these problems strength data were obtained by determining the pH values for 50% loading of copper from stripping experiments in which chloroform solutions of preformed [Cu(**L**-H)$_2$] were contacted with aqueous solutions having different acidities but a constant sulfate (0.01 M) concentration. The pH-dependence of copper loading curves and pH$_{0.5}$ values are shown in Figure 10.

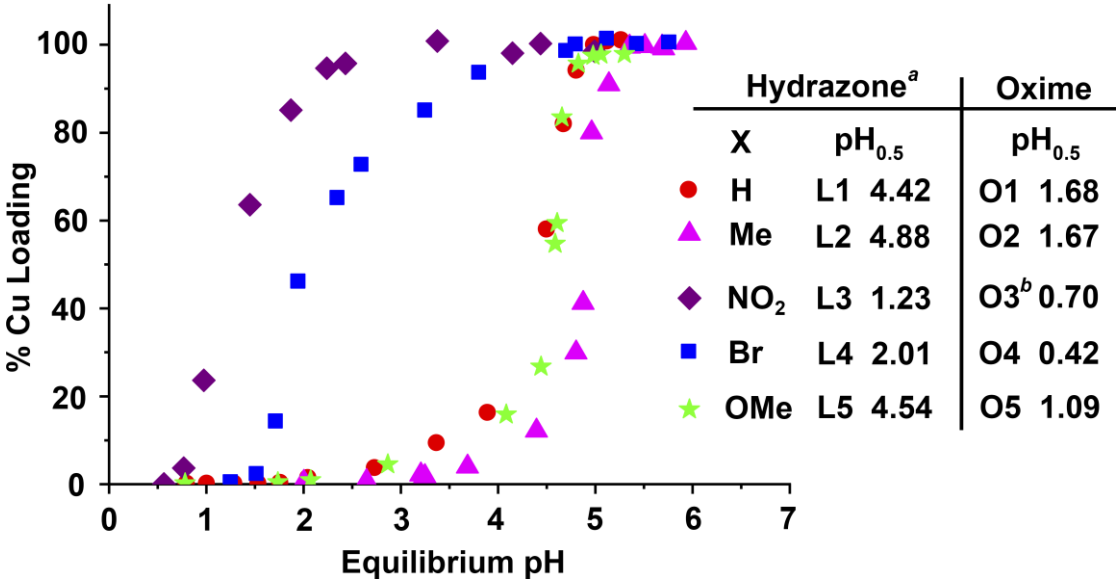

Figure 10 Copper loading of **L1**-**L5** after contacting 0.005 M chloroform solutions of [Cu(**L**-H)$_2$] with an equal volume 0.01 M Na_2SO_4 aqueous solutions of various acidities. The $pH_{0.5}$ values of the oxime analogues **O1**-**O5** are also listed.
[a] For [Cu(**L3**-H)$_2$], 0.0005 M chloroform solutions were used due to the limited solubility. [b] Value for the 5-*t*-octyl-substituted analogue as **O4** and its copper complex have insufficient solubility to allow the experiment to be conducted.

Clearly 3-substitution significantly affects the extraction strength and the distribution coefficient for copper transfer varies by more than three orders of magnitude across the series: NO_2 > Br > H ≥ OMe ≥ Me. It is apparent that the hydrazones are intrinsically weaker extractants than their oxime analogues ($pH_{0.5}$ data[6] for the latter, **O1**-**O5**, are included for comparison in the table inset in Figure 10). The unsubstituted hydrazone (**L1**) and its 3-methyl and 3-methoxy derivatives (**L2** and **L5**) show distribution coefficients for Cu^{II} approximately three orders of magnitude smaller than their oxime analogues (**O1**, **O2** and **O5**). The differences in strength between the 3-nitro- and 3-bromo-substituted hydrazones **L3** and **L4** and their oxime analogues (**O3** and **O4**), and between all the oximes (**O1**-**O5**) is much smaller.

In an attempt to define to what extent the electronic, steric and hydrogen bond buttressing properties of the 3-X substituents determine the relative strengths of the extractants DFT calculations were carried out to determine the enthalpies of the reactions

$$2L_g + Cu^{2+}{}_g \rightarrow [Cu(L\text{-}H)_2]_g + 2H^+{}_g \qquad \textbf{Equation 6}$$

and

$$[L]_{2g} + Cu^{2+}{}_g \rightarrow [Cu(L\text{-}H)_2]_g + 2H^+{}_g \text{ (see Table 3).} \qquad \textbf{Equation 7}$$

	L1 X = H	**L3** X = NO_2	**L4** X = Br	**L5** X = OMe	**O1** X = H
E_{depr}/kcal mol^{-1} for L→$[L\text{-}H]^- + H^+$ [a]	364.48	347.32	357.19	364.84	356.42
E_{dimer}/kcal mol^{-1}, $[L]_2$ [a]	-8.46	-17.08	-11.98	-10.92	-10.63
E_{form}/kcal mol^{-1}, $[Cu(L\text{-}H)_2]$ from $[L]_2$ [a]	34.57	30.44	33.08	32.80	27.43
E_{form}/kcal mol^{-1}, $[Cu(L\text{-}H)_2]$ from 2L [a]	26.11	13.36	21.10	21.88	16.80
NBO for Cu-O /kcal mol^{-1} [b]	51.23	52.01	52.69	54.7	50.10
NBO for Cu-N /kcal mol^{-1} [b]	36.71	37.07	36.05	37.26	47.37
Torsion angle O-Cu-N-Y/° [b]	170.5	172.5	174.2	171.9	179.98
Torsion angle O'-Cu-N-Y/° [b]	9.47	7.48	5.84	8.10	0.01
NBO for Y-H…O/kcal mol^{-1} [b]	9.13	5.77	5.98	6.08	11.5
Y-H…O contact distance/Å [b]	1.86	1.91	1.88	1.86	1.78
Y-H…X contact distance/Å [b]	2.91	2.02	2.81	2.72	2.99
Distance of Y from the least squares mean plane CuN_2O_2/Å [b]	0.21	0.16	0.13	0.18	0.00

Table 3 DFT calculated gas phase deprotonation enthalpies (E_{depr}, L → $[L\text{-}H]^- + H^+$), ligand dimerization energies(E_{dimer}, 2L → $[L]_2$), Cu complex formation energies, natural bond orders (NBO) and geometric data for energy-minimised structures of Cu complexes.
[a, b] Energies and Cartesian coordinates for energy-minimised structures are provided in the ESI, sections 4.1 and 4.2 respectively.

The energy-minimised structures of the copper complexes (see ESI) compare closely with those determined by X-ray crystallography. As for the X-ray structures (Table 2), the DFT calculations indicate that the N-N bonds in the hydrazone complexes are bent away from the coordination plane. In contrast, the N-O bonds in the oxime [Cu(**O1**-$H)_2$] lie very close to the CuN_2O_2 plane (see O-Cu-N-Y torsion angles in Table 3). This is consistent with the interligand O-H···$O_{phenolate}$ hydrogen bonds being shorter and stronger than the N-H···$O_{phenolate}$ hydrogen bonds in the hydrazone complexes. The greater strength of the hydrogen bonds to the phenolate oxygen atoms in [Cu(**O1**-$H)_2$] is consistent with the oxime complex having slightly weaker Cu-O bonds than those in the hydrazone complexes (see natural bond order values in Table 3).

The buttressing of interligand hydrogen bonding by the nitro-, bromo- and methoxy-groups in [Cu(**L3**-$H)_2$], [Cu(**L4**-$H)_2$] and [Cu(**L3**-$H)_2$] (see the Y-H…X contact distances, Table 3) is, as might be expected, accompanied by a weakening of the other interligand hydrogen bond (Y-H…$O_{phenolate}$).

The non-planar disposition of bonds about the coordinated nitrogen atoms in the hydrazone complexes suggests that they have sp^3 character to a greater extent than those in their oxime analogue. This is associated with them forming significantly weaker Cu-N bonds than those in the oxime complex [Cu(**O1**-$H)_2$] and mirrors the relative Cu-N bond lengths found in the solid state structures (see table 2).

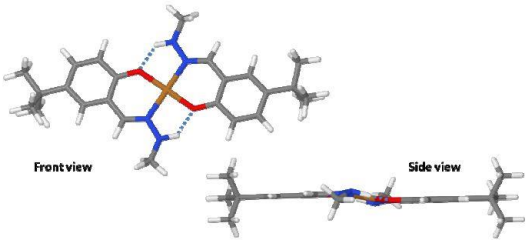

Figure 4.26: Energy minimised structure for the complex [Cu(**L9**)$_2$] with inter-molecular hydrogen bonding highlighted (blue). The side view illustrates reduced planarity of the complex (with respect to oxime analogues) arising from its non planar N-NHMe groups.

Figure 11 The calculated structure of [Cu(**L1**-H)$_2$] showing the displacement of the N-NHMe uits from the coordination plane.

The extent to which the 3-X substituents can buttress the inter-ligand hydrogen bonds is also revealed by the enthalpies of formation of the proligand dimers (E_{dimer} in Table 3). Incorporation of the hydrogen bond accepting groups, NO_2, Br and OMe, leads to more favourable enthalpies of dimerisation than that for the unsubstituted compound.

As discussed above, the NO_2, Br and OMe groups all show bonding interactions in the outer coordination sphere with the hydrazone hydrogen. Although the nitro-substituent forms a particularly strong interaction with the hydrazone N-H group the dimerization enthalpy of **L3** is only slightly more favourable than that of the unsubstituted ligand **L1**. This is a consequence of the monomer adopting a very favourable conformation which allows the phenolic OH group to hydrogen bond to the adjacent nitro substituent and the hydrazone N-H group to the phenolic oxygen atom.

The calculated gas phase formation energies for the copper complexes ($[L]_{2(g)} + Cu^{2+}_{(g)} = [Cu(L\text{-}H)_2]_{(g)} + 2H^+_{(g)}$, Table 3) are all more favourable for the hydrogen bond acceptor groups, NO_2, Br and OMe. This trend is not so marked for the methoxy-substituted ligand, mainly a consequence of its less favourable deprotonation enthalpy. Whilst the predicted order of extractant strength, $NO_2 > Br > OMe > H$, appears to correlate reasonably well with that observed experimentally, $NO_2 > Br > H \geq OMe$, the calculated values are based on the assumption that the reagents are exclusively in the cyclic dimeric form prior to copper uptake, and this is known not to be the case for the nitro ligand **L3** (see above). If the monomeric proligands are taken as the starting forms, the nitro-substituted extractant still shows the most favourable formation energy.

For **L5**, the electron-donating properties of the methoxy substituent lead to a higher deprotonation enthalpy term than for the unsubstituted ligand **L1**, but this appears to be more than compensated by the more favourable strengths of bonds to copper and the buttressed hydrogen bonding to the hydrazone NH.

At first sight the correlation between calculated energies of formation in the gas phase and the relative strength of extractants in a two phase liquid system is quite remarkable. As discussed recently for other systems where this occurs,[62] this correlation will only

be observed when the process occurring in the aqueous phase is the same, in this case two protons replacing one copper dication, for the series of extractions. Consequently, as in this work, hydration energies of species do not contribute to *differences* in the formation energies of metal complexes. The solvation energies of the proligands and their copper complexes in the organic phase will obviously show some dependence on the nature of the 3-X substituent. However, the *differences* in solvation energies particularly of the preorganised dimers and their copper complexes are likely to be fairly small and consequently it is the effect of the 3-X substituents on the deprotonation energies of the proligands and the binding energies of the conjugate anions to copper which largely determine the energies of formation of the complexes.

Conclusions

The approach of using the cavity size in macrocyclic ligands to tune the strength of binding of base metal ions, established by Lindoy and co-workers,[63] can be extended to much simpler reagents such as the salicylaldehyde hydrazone ligands described in this work which assemble in *pseudo*macrocyclic structures *via* interligand hydrogen bonding.

The N-methyl hydrazone derivatives (**L1-L5**) are analogues of the commercial phenolic oxime reagents but are significantly weaker copper extractants. On the basis of the DFT calculations and X-ray structure determinations it appears that this arises from a combination of the weaker Cu-N bonds and the less favourable inter-ligand hydrogen bonds formed by the hydrazones (OH groups are generally better hydrogen bond donors than NH groups[64,65]) and from their higher deprotonation enthalpies. The *N*-phenyl hydrazones (**L6-L10**) are too weak to allow solvent extraction to be carried out under conventional conditions.

The results confirm the importance of understanding outer sphere coordination chemistry in designing metal solvent extractants and in particular the efficacy of interligand hydrogen bonding in extracted species. As for the oximes,[6,7] the introduction of substituents adjacent to the phenolic hydroxyl group with electron withdrawing and hydrogen bond acceptor properties significantly increases the strength as copper extractants. For the *N*-methyl hydrazones the distribution coefficient for copper extraction is increased by three orders of magnitude on introducing a 3-bromo or 3-nitro-substituent. The resulting extractants have strengths comparable to the commercial oximes, but their lower solubilities in water-immiscible solvents and the higher costs of synthesis arising from introduction of the substituent make them poor candidates to replace the tried and tested commercial reagents.

161102 Master copy to RSF with new Table 2 and Fig 10.

Experimental

Chemicals and Equipment: Unless otherwise specified a reagent or solvent was used as obtained from Aldrich, Fisher or Acros. Standards for inductively coupled plasma optical emission spectroscopy (ICP-OES) were purchased from Alfa Aesar. ^{1}H and ^{13}C NMR spectra recorded in the experimental section were run on a Bruker ARX250 at ambient temperature. ^{1}H NMR NOESY spectra were recorded on a Bruker DPX360 spectrometer at 298 K (unless stated otherwise), and chemical shifts (δ) are reported in parts per million (ppm) relative to TMS. CHN analytical data were obtained by the University of St Andrews Microanalytical Service. Mass spectrometry was performed on a Micromass ZMD instrument with a z-spray ESI source. Melting points were measured on a Gallenkamp melting point apparatus. ICP-OES analysis was performed on a Perkin Elmer Optima 5300DV spectrometer. The measurement of pH was carried out using a Sartorius PP-50 pH-meter.

X-ray crystal structures were obtained by measuring suitably sized crystals on either a Bruker D8 with a Smart Apex or Apex II CCD or an Oxford Diffraction SuperNova with an Atlas CCD. Data were collected at 150K unless otherwise specified and reduced with the relevant manufacturer's software. All structures were solved by direct methods and refined with ShelXL. Refer to ESI for the details for each structure.

NMR Studies: Samples were generally prepared by dissolving 10 mg the ligand in 0.6 ml $CDCl_3$ or DMSO-d_6. Samples for NOESY and 1D NOE difference spectra required more concentrated solutions, and 40 mg the ligand in 0.6 ml $CDCl_3$ were used. The concentration dependence NMR study was carried out by diluting a NMR sample containing 40 mg the ligand in 0.6 ml DMSO-d_6 to respectively 1.2 ml, 1.6 ml and 2.4 ml in the same NMR tube

Solvent Extraction: Preliminary loading experiments were carried out by contacting a chloroform solution of the ligand (5.00 ml, 0.010 M) with an aqueous solution of copper(II) sulfate (5.00 ml, 0.010 M) at different pH values in a tightly sealed, screw top glass jar. The aqueous solution was prepared by adding a H_2SO_4 solution (0.10 M for pH 1.5 and above, 1.00 M for lower pH) or a NaOH solution (0.10 M) to a $CuSO_4$ solution (3.00 ml, 0.0167 M) and adding water to make up to 5.00 ml. The two-phase system was stirred at 900 r.p.m. at room temperature for 18 h. A 1.00 ml aliquot was taken from the organic phase, dried *in vacuo* and redissolved in butan-1-ol (10.00 ml). The residues from **L3** and **L4** solutions were dissolved in nitrobenzene. The copper was then analysed by ICP-OES. The pH of the aqueous phase was measured using a pH meter. The calculated percentage of the copper(II) taken into the organic phase was plotted against the measured equilibrium pH to give the S-curve.

The data presented in Figure 10 were obtained by taking a chloroform solution of the copper(II) complex (5.00 ml, 0.005 M) and an aqueous solution of sodium sulfate (5.00 ml, 0.010 M) with varied H_2SO_4 content. In some cases the low solubility of the complex required slight modifications of the procedure, (see section 3 in ESI).

Computational work: For the determination of energies of formation (rows 1-4 in Table 3) DFT calculations employed the B3LYP hybrid exchange-correlation functional[66,67] and the 6-31+G(d,p) basis set,[68-71] and were performed using the Gaussian 09 Revision E.01 program.[72] The energy-minimised structures used to

compare bond lengths and angles and to provide NBO data (rows 5-12 in Table 3) were generated using Gaussian 03[73] with the B3LYP functional and 6-31G+(d,p) basis set. More information, including Cartesian coordinates for atom positions, are provided in Tables S4.1 and S4.2 in the ESI.

Synthesis: The preparation and characterisation of all ligands and copper complexes are described in detail in the ESI (section 5).

Acknowledgments

We thank the EPSRC for funding, EaStCHEM for the award of a studentship to TL and for access to the EaStCHEM Research Computing Facility, Cytec Industries and Infineum UK for funding of PhD studentships for RSF, BDR and FJW and Ron Swart and John Campbell of Cytec Industries for helpful discussions.

References

[1] P. J. Mackey, *CIM Magazine*, **2007**, *2*, 35-42.
[2] Michael Moser, *Personal Communication*, Cytec Solvay Group, Stamford, CT 06904, USA.
[3] A. M. Wilson, P. J. Bailey, P. A. Tasker, J. R. Turkington, R. A. Grant, J. B. Love, *Chem. Soc. Rev.*, **2014**, *43*, 123-134.
[4] P. A. Tasker, P. G. Plieger, L. C. West, *Comprehensive Coordination Chemistry II*, Elsevier Ltd, Oxford, **2004**.
[5] A. G. Smith, P. A. Tasker, D. J. White, *Coord. Chem. Rev.*, **2003**, *241*, 61-85.
[6] R. S. Forgan, B. D. Roach, P. A. Wood, F. J. White, J. Campbell, D. K. Henderson, E. Kamenetzky, F. E. McAllister, S. Parsons, E. Pidcock, P. Richardson, R. M. Swart, P. A. Tasker, *Inorg. Chem.* **2011**, *50*, 4515–4522.
[7] R. S. Forgan, P. A. Wood, J. Campbell, D. K. Henderson, F. E. McAllister, S. Parsons, E. Pidcock, R. M. Swart, P. A. Tasker, *Chem. Commun.*, **2007**, 4940-4942.
[8] J. Szymanowski, A. Borowiak-Resterna, *Crit. Rev. Anal. Chem.*, **1991**, *22*, 519-566.
[9] K. Burger, I. Egyed, *J. Inorg. Nucl. Chem.*, **1965**, *27*, 2361-2370.
[10] K. Burger, I. Egyed, *Magy. Kem. Foly.*, **1965**, *71*, 143-149.
[11] J. Bernstein, R. E. Davis, L. Shimoni, N.-L. Chang, *Angew. Chem. Int. Ed.*, **1995**, *34*, 1555-1573.
[12] R. B. Singh, P. Jain, R. P. Singh, *Talanta*, **1982**, *29*, 77-84.
[13] M. P. Jain, S. Kumar, *Indian J. Chem., Sect. A*, **1978**, *16A*, 464-465.
[14] L. Hunter, J. A. Marriott, *J. Chem. Soc.*, **1937**, 2000-2003.
[15] T. V. Troepol'skaya, E. N. Munin, Z. S. Titova, Y. P. Kitaev, *Izv. Akad. Nauk SSSR, Ser. Khim.*, **1978**, 898-905.
[16] R. S. Mandal, L. Mishra, *Asian J. Chem.*, **2007**, *19*, 95-101.
[17] M. P. Jain and S. Kumar, *Talanta*, **1982**, *29*, 52-53.
[18] N. Guskos, V. Likodimos, S. Glenis, J. Typek, M. Wabia, D. G. Paschalidis, I. Tossidis, C. L. Lin, *J. Magn. Magn. Mater.*, **2004**, *272-276*, 1067-1069.
[19] S. N. Rao, D. D. Mishra, R. C. Maurya, N. N. Rao, *Polyhedron*, **1997**, *16*, 1825-1829.
[20] L. Larabi, Y. Harek, A. Reguig, M. M. Mostafa, *J. Serb. Chem. Soc.*, **2003**, *68*, 85-95.

[21] F. Cariati, U. Caruso, R. Centore, W. Marcolli, A. De Maria, B. Panunzi, A. Roviello, A. Tuzi, *Inorg. Chem.*, **2002**, *41*, 6597-6603.
[22] P. G. Lacroix, *Eur. J. Inorg. Chem.*, **2001**, 339-348.
[23] U. Caruso, R. Centore, B. Panunzi, A. Roviello, A. Tuzi, *Eur. J. Inorg. Chem.*, **2005**, 2747-2753.
[24] B.-D. Wang, Z.-Y. Yang, D.-W. Zhang, Y. Wang, *Spectrochim. Acta, Part A*, **2006**, *63A*, 213-219.
[25] A. Majumder, G. M. Rosair, A. Mallick, N. Chattopadhyay, S. Mitra, *Polyhedron*, **2006**, *25*, 1753-1762.
[26] Y. Xiang, Z. Li, X. Chen, A. Tong, *Talanta*, **2008**, *74*, 1148-1153.
[27] M. Bakir, C. Gyles, *J. Mol. Struct.*, **2005**, *753*, 35-39.
[28] D. K. Johnson, T. B. Murphy, N. J. Rose, W. H. Goodwin, L. Pickart, *Inorg. Chim. Acta*, **1982**, *67*, 159-165.
[29] J. E. Dubois, H. Fakhrayan, J. P. Doucet, J. M. El Hage Chahine, *Inorg. Chem.*, **1992**, *31*, 853-859.
[30] M. Mohan, A. Kumar, M. Kumar and N. K. Jha, *Inorganica Chimica Acta*, 1987, **136**, 65-74.
[31] E. W. Ainscough, A. M. Brodie, A. J. Dobbs, J. D. Ranford and J. M. Waters, *Inorganica Chimica Acta*, 1998, **267**, 27-38.
[32] M. Alagesan, N. S. P. Bhuvanesh, N. Dharmaraj, *Dalton Trans.*, **2013**, *42*, 7210-7223.
[33] X.-P. Ye, T.-F. Zhu, W.-N. Wu, T.-L. Ma, J. Xu, Z.-P. Zhang, Y. Wang, L. Jia, *Inorg. Chem. Commun.*, **2014**, *47*, 60-62.
[34] J. Patole, U. Sandbhor, S. Padhye, D. N. Deobagkar, C. E. Anson, A. Powell, *Bioorg. Med. Chem. Lett.*, **2003**, *13*, 51–55.
[35] A. Jamadar, A.-K. Duhme-Klair, K. Vemuri, M. Sritharan, P. Dandawate, S. Padhye, *Dalton Trans.*, **2012**, *41*, 9192-9201.
[36] E. Massarani, D. Nardi, A. Tajana, L. Degen, *J. Med. Chem.*, **1971**, *14*, 633-635.
[37] P. B. Sreeja, M. R. P. Kurup, A. Kishore, C. Jasmin, *Polyhedron*, **2004**, *23*, 575-581.
[38] J. K. Sears, J. R. Darby, *The Technology of Plasticizers*, John Wiley and Sons, New York, **1982**.
[39] A. M. El-Hendawy, A. H. Al-Kubaisi, A. F. Shoair, *Monatsh. Chem.*, **1995**, *126*, 1291-1302.
[40] T. Mino, T. Ogawa, M. Yamashita, *Heterocycles*, **2001**, *55*, 453-456.
[41] T. Mino, Y. Shirae, M. Sakamoto, T. Fujita, *J. Org. Chem.*, **2005**, *70*, 2191-2194.
[42] M. F. Iskander, T. E. Khalil, R. Werner, W. Haase, I. Svoboda, H. Fuess, *Polyhedron*, **2000**, *19*, 949-958.
[43] N. M. Samus, V. I. Tsapkov, A. V. Kerner, *Russ. J. Gen. Chem.*, **2003**, *73*, 1611-1615.
[44] N. M. Samus, V. I. Prisakar, V. I. Tsapkov, S. A. Buracheva, A. P. Gulya, *Pharm. Chem. J.*, **2004**, *38*, 373-375.
[45] S. Das, S. Pal, *J. Mol. Struct.*, **2005**, *753*, 68-79.
[46] L.-M. Wu, H.-B. Teng, X.-C. Feng, X.-B. Ke, Q.-F. Zhu, J.-T. Su, W.-J. Xu, X.-M. Hu, *Cryst. Growth Des.*, **2007**, *7*, 1337-1342.
[47] R. J. Gordon, J. Campbell, D. K. Henderson, D. C. R. Henry, R. M. Swart, P. A. Tasker, F. J. White, J. L. Wood, L. J. Yellowlees, *Chem. Commun.*, **2008**, 4801-4803.
[48] R. J. Gordon, J. Campbell, D. C. R. Henry, R. M. Swart, P. A. Tasker, F. J. White, J. L. Wood, L. J. Yellowlees. *Proceedings of the International Solvent Extraction Conference*, Tucson, Arizona, **2008**, 1475.

[49] R. Aldred, R. Johnston, D. Levin, J. Neilan, *J. Chem. Soc., Perkin Trans. 1*, **1994**, 1823-1831.
[50] F. Lam, J. X. Xu, K. S. Chan, *J. Org. Chem.*, **1996**, *61*, 8414-8418.
[51] D. F. Taber, S. Patel, T. M. Hambleton, E. E. Winkel, *J. Chem. Educ.*, **2007**, *84*, 1158.
[52] L. F. Lindoy, G. V. Meehan, N. Svenstrup, *Synthesis*, **1998**, 1029-1032.
[53] J. Clayden, N. Greeves, S. Warren, W. Peter, *Organic Chemistry*, Oxford University Press, Oxford, **2001**.
[54] V. A. Bren, T. M. Stul'neva, B. Y. Simkin, V. I. Minkin, *Zh. Org. Khim.*, **1976**, *12*, 633-640.
[55] G. Socrates, *Trans. Faraday Soc.*, **1970**, *66*, 1052-1057.
[56] Y. Tsuno, M. Fujio, Y. Takai, Y. Yukawa, *Bull. Chem. Soc. Jpn.*, **1972**, *45*, 1519-1529.
[57] D. H. Williams, I. Fleming, *Spectroscopic Methods in Organic Chemistry*, McGraw-Hill Publishing Company, London, **1995**.
[58] J. B. Hyne, *Can. J. Chem.*, **1960**, *38*, 125-130.
[59] M. Onda, Y. Yamamoto, Y. Inoue, R. Chujo, *Bull. Chem. Soc. Jpn.*, **1988**, *61*, 4015-4021.
[60] S. H. Gellman, G. P. Dado, G. B. Liang, B. R. Adams, *J. Am. Chem. Soc.*, **1991**, *113*, 1164-1173.
[61] G. T. Crisp, Y.-L. Jiang, *ARKIVOC*, **2001**, *2*, 77-87.
[62] M. R. Healy, J. W. Roebuck, E. D. Doidge, L. C. Emeleus, P. J. Bailey, J. Campbell, A. J. Fischmann, J. B. Love, C. A. Morrison, T. Sassi, D. J. White, P. A. Tasker, *Dalton Trans*., **2016**, *45*, 3055-3062.
[63] K. Henrick, P. A. Tasker, L. F. Lindoy, *Prog .Inorg .Chem*., **1985**, *33*, 1-58
[64] P. A. Kollman, L. C. Allen, *Chem. Rev.*, **1972**, *72*, 283-303.
[65] H. Umeyama, K. Morokuma, *J. Am. Chem. Soc.*, **1977**, *99*, 1316-1332.
[66] A. D. Becke, *J. Chem. Phys.*, **1993**, *98*, 5648-5652.
[67] P. J. Stephens, F. J. Devlin, C. F. Chabalowski, M. J. Frisch, *J. Phys. Chem.*, **1994**, *98*, 11623-11627.
[68] W. J. Hehre, R. Ditchfield, J. A. Pople, *J. Chem. Phys.*, **1972**, *56*, 2257-2261.
[69] P. C. Hariharan, J. A. Pople, *Theor. Chim. Acta*, **1973**, *28*, 213-222.
[70] T. Clark, J. Chandrasekhar, G. W. Spitznagel, P. V. R. Schleyer, *J. Comput. Chem.*, **1983**, *4*, 294-301.
[71] V. A. Rassolov, M. A, Ratner, J. A. Pople, P. C. Redfern, L. A. Curtiss, *J. Comput. Chem.*, **2001**, *22*, 976-984.
[72] M. J. Frisch, G. W. Trucks, H. B. Schlegel, G. E. Scuseria, M. A. Robb, J. R. Cheeseman, G. Scalmani, V. Barone, B. Mennucci, G. A. Petersson, H. Nakatsuji, M. Caricato, X. Li, H. P. Hratchian, A. F. Izmaylov, J. Bloino, G. Zheng, J. L. Sonnenberg, M. Hada, M. Ehara, K. Toyota, R. Fukuda, J. Hasegawa, M. Ishida, T. Nakajima, Y. Honda, O. Kitao, H. Nakai, T. Vreven, J. A. Montgomery, Jr., J. E. Peralta, F. Ogliaro, M. Bearpark, J. J. Heyd, E. Brothers, K. N. Kudin, V. N. Staroverov, R. Kobayashi, J. Normand, K. Raghavachari, A. Rendell, J. C. Burant, S. S. Iyengar, J. Tomasi, M. Cossi, N. Rega, J. M. Millam, M. Klene, J. E. Knox, J. B. Cross, V. Bakken, C. Adamo, J. Jaramillo, R. Gomperts, R. E. Stratmann, O. Yazyev, A. J. Austin, R. Cammi, C. Pomelli, J. W. Ochterski, R. L. Martin, K. Morokuma, V. G. Zakrzewski, G. A. Voth, P. Salvador, J. J. Dannenberg, S. Dapprich, A. D. Daniels, Ö. Farkas, J. B. Foresman, J. V. Ortiz, J. Cioslowski, D. J. Fox, *Gaussian 09, Revision E.01*, Gaussian, Inc., Wallingford CT, 2009.
[73] M. J. Frisch, G. W. Trucks, H. B. Schlegel, G. E. Scuseria, M. A. Robb, J. R.

Cheeseman, J. A. Montgomery, Jr., T. Vreven, K. N. Kudin, J. C. Burant, J. M. Millam, S. S. Iyengar, J. Tomasi, V. Barone, B. Mennucci, M. Cossi, G. Scalmani, N. Rega, G. A. Petersson, H. Nakatsuji, M. Hada, M. Ehara, K. Toyota, R. Fukuda, J. Hasegawa, M. Ishida, T. Nakajima, Y. Honda, O. Kitao, H. Nakai, M. Klene, X. Li, J. E. Knox, H. P. Hratchian, J. B. Cross, V. Bakken, C. Adamo, J. Jaramillo, R. Gomperts, R. E. Stratmann, O. Yazyev, A. J. Austin, R. Cammi, C. Pomelli, J. W. Ochterski, P. Y. Ayala, K. Morokuma, G. A. Voth, P. Salvador, J. J. Dannenberg, V. G. Zakrzewski, S. Dapprich, A. D. Daniels, M. C. Strain, O. Farkas, D. K. Malick, A. D. Rabuck, K. Raghavachari, J. B. Foresman, J. V. Ortiz, Q. Cui, A. G. Baboul, S. Clifford, J. Cioslowski, B. B. Stefanov, G. Liu, A. Liashenko, P. Piskorz, I. Komaromi, R. L. Martin, D. J. Fox, T. Keith, M. A. Al-Laham, C. Y. Peng, A. Nanayakkara, M. Challacombe, P. M. W. Gill, B. Johnson, W. Chen, M. W. Wong, C. Gonzalez, and J. A. Pople, *Gaussian 03, Revision E.01,* Gaussian, Inc., Wallingford CT, 2004.